Analysis method for quantifying the morphology of nanotube networks

Vobornik, Dusan; Zou, Shan; Lopinski, Gregory P.

Publisher's version / Version de l'éditeur:
https://doi.org/10.1021/acs.langmuir.6b02475
Langmuir, 32, 34, pp. 8735-8742, 2016-08-10

LANGMUIR

Article

pubs.acs.org/Langmuir

Analysis Method for Quantifying the Morphology of Nanotube Networks

Dusan Vobornik,* Shan Zou, and Gregory P. Lopinski

Measurement Science and Standards, National Research Council Canada, 100 Sussex Drive, Ottawa, Ontario K1A 0R6, Canada

Supporting Information

ABSTRACT: While atomic force microscopy (AFM) is a powerful technique for imaging assemblies and networks of nanoscale materials, approaches for quantitative assessment of the morphology of these materials are lacking. Here we present a volume-based approach for analyzing AFM images of assemblies of nano-objects that enables the extraction of relevant parameters describing their morphology. Random networks of single-walled carbon nanotubes (SWCNTs) deposited via solution-phase processing are used as an example to develop the method and demonstrate its utility. AFM imaging shows that the morphology of these networks depends on details of processing and is influenced by choice of substrate, substrate cleaning method, and postdeposition rinsing protocols. A method is outlined to analyze these images and extract relevant parameters describing the network morphology such as the density of SWCNTs and the degree to which tubes are bundled. Because this volume-based approach depends on accurate measurements of the height of individual tubes and their networks, a procedure for obtaining reliable height measurements is also discussed. Obtaining quantitative parameters that describe the network morphology allows going beyond qualitative descriptions of images and will facilitate optimizing network preparation methods based on measurable criteria and correlating performance with morphology.

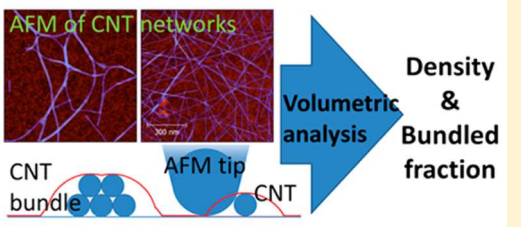

INTRODUCTION

Nano-objects such as nanotubes, nanowires, nanosheets, and nanoparticles continue to be of interest as building blocks for functional materials due to their remarkable size-dependent properties. However, the properties of materials constructed from these objects depend not only on the properties of the objects themselves but also on how these blocks assemble into larger structures.[1−3] Although electron and scanned probe microscopies are commonly used to visualize the morphology of these assemblies, methods for quantitative assessment of the resulting images have received less attention. Extraction of quantitative parameters describing the morphology of a sample from images will facilitate feedback on how processing affects the structure and ultimately how the structure influences the properties of the material.

While the analysis approach presented here should be widely applicable to a range of nanoscale materials, random networks of single-walled carbon nanotubes deposited from solution are used as an example to illustrate the method and demonstrate its utility. These networks represent interesting model systems for investigating the interplay between the intrinsic properties of the individual nanoscale building blocks and process-dependent network morphologies in determining properties. While individual single-walled carbon nanotubes (SWCNTs) exhibit high intrinsic conductivities and field effect mobilities, films based on random networks of these tubes show considerably lower values.[1,4−7] Over distances greater than the length of an individual tube, electrical transport is usually limited by tube−tube junctions, making the conductivity highly dependent on details of the network morphology (i.e., tube density, bundling, and alignment).[8−12] Furthermore, starting with the same carbon nanotube ink, process details can strongly influence the morphology and consequently the electronic properties of the network.[13]

Atomic force microscopy (AFM) is a powerful and versatile probe of nanomaterial morphologies, enabling imaging of the individual nano-objects and their assemblies in a variety of environments (vacuum, ambient, liquid) and regardless of whether these materials are insulating or conducting. Quantitative AFM studies of nanomaterials have typically focused on extracting distributions of lengths, heights, or diameters for individual nano-objects.[14−19] Obtaining this type of data usually requires optimizing sample preparation conditions so that isolated features can be imaged on a flat substrate. However, functional assemblies are most often achieved at higher densities. For example, the formation of conductive networks of nanowires and nanotubes for applications such as transparent conductive electrodes or channel materials for thin film transistors (TFTs) requires densities above the percolation threshold. At these higher densities there is likely to be some degree of overlap and aggregation of the individual building blocks. In these realistic applications it is often hard to see where one nano-object ends and the other starts, making it difficult to accurately count the

Received: July 4, 2016
Revised: August 5, 2016

exact number of objects in the network. Among several measurands that can be used to characterize the morphology of a random network of nanowires or tubes, two that are particularly important in determining electronic and optical properties are the tube density and the extent to which the individual tubes aggregate into bundles. In this work a straightforward and fast volume-based method to extract these measurands from experimentally obtained AFM images is presented. The use of a volume-based analysis method means that the accuracy of AFM height measurements (from which the volume is calculated) is of paramount importance. Therefore, we also propose an experimental procedure that facilitates verification of the AFM imaging parameters to ensure reliable measurements of the nanotube height.

EXPERIMENTAL SECTION

Substrate Preparation. Two different substrates were used; a thermally grown SiO_2 thin film on silicon, and highly ordered pyrolytic graphite (HOPG). A silicon wafer with a 100 nm thick thermal oxide (Silicon Quest International) was cut into 1 cm^2 pieces. Prior to nanotube network deposition the silicon oxide surface was cleaned by either: (a) Piranha solution bath (3:1 volume ratio of 98% H_2SO_4 and 30% H_2O_2) for 30 min, followed by thorough rinsing with ultrapure water (resistivity of 18.2 MΩ·cm), and blown dry with nitrogen; or (b) 5 min in an oxygen plasma cleaner (Yield Engineering Systems G-500). For the HOPG substrates, we used ZYB-grade, 12 mm × 12 mm HOPG squares (Bruker AFM Probes, Camarillo, CA). Clean surfaces were obtained by cleaving off the top layers with Scotch tape prior to nanotube network deposition.

SWCNT Network Preparation. A commercially available ultra-high purity semiconducting SWCNT dispersion was purchased from Nanointegris (http://www.nanointegris.com/IsoSol-S100). The separation and purity of these nanotubes are ensured by the poly(9,9-di-*n*-dodecylfluorene) (PFDD) wrapping.[20] Networks were prepared by dropcasting 40 μL of a 10 mg/L toluene solution of the nanotubes on clean substrates and letting the toluene evaporate. This typically took 10 to 15 min. To remove excess polymer (initial polymer to nanotube mass ratio was 4 to 1), as well as any other contaminants, we rinsed the samples upon solvent evaporation with a steady stream of toluene for 20 s or by successive 20 s rinses of toluene, tetrahydrofuran (THF), and isopropanol (IPA). Finally, samples were dried with nitrogen and stored in a closed Petri dish under room conditions. AFM measurements were carried within a day of preparation, but several samples were again measured at different times during several months following their preparation with no significant changes in morphology observed.

Chemicals. Toluene and tetrahydrofuran were purchased from EMD Millipore with respective purities (GC) of ≥99.5 and ≥99.9%. Distilled in glass-grade isopropanol was purchased from Caledon Chemicals with a purity (GC) of ≥99.7%.

AFM Imaging. The samples were imaged using the MultiMode AFM with the NanoScope V controller (Bruker Nano Surfaces Division, Santa Barbara, CA) in Bruker's proprietary PeakForce QNM mode. The peak force with which the tip taps the sample surface was always kept close to the lowest stable imaging level of 0.5 nN or less (stable here means perfectly overlapped trace and retrace lines during AFM scanning). We have used ScanAsyst-Air AFM probes (Bruker AFM Probes, Camarillo, CA), which are made of silicon nitride and whose typical tip radius is 2 nm according to the manufacturer's specifications.

Analysis Software. All analysis of AFM images was performed using Gwyddion, a free, open-source software, with well-defined and explained operations and functions.[21]

RESULTS AND DISCUSSION

Process Details Influence SWCNT Network Morphology. AFM images of SWCNT networks processed in slightly different ways are shown in Figure 1. The rather different morphologies readily apparent in these images illustrate how

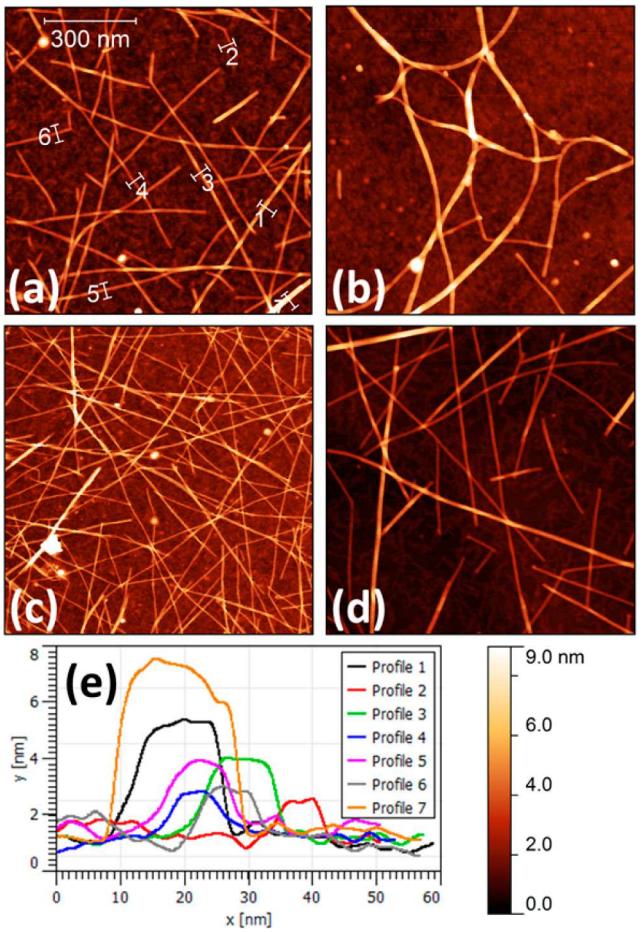

Figure 1. AFM images of networks obtained by dropcasting the same solution of carbon nanotubes on SiO_2 (a−c) and HOPG (d). Prior to deposition, SiO_2 substrates were cleaned either by Piranha solution (a,b) or by oxygen plasma treatment (c), while HOPG was freshly cleaved (d). Upon solvent evaporation samples were rinsed with toluene for 20 s (a,c,d) or sequentially with toluene, tetrahydrofuran, and isopropanol for 20 s each (b). All images have the same 1 μm^2 size and are displayed with the same 9 nm vertical scale, where 0 corresponds to the lowest pixel height in the image. Cross sections in panel e correspond to numbered lines shown in panel a.

details of sample processing influence network formation, even starting from the same SWCNT dispersion. Specifically, the observed network variations result from the use of different substrates, different substrate cleaning procedures, or different postdeposition rinsing procedures, as detailed in the figure caption. It is easy to qualitatively observe certain differences between the networks in Figure 1. For example, there seems to be more tubes on the oxygen plasma-cleaned (Figure 1c) versus piranha-cleaned SiO_2 surface (Figure 1a). Similarly, it appears that additional rinsing with tetrahydrofuran and isopropanol (Figure 1b) leads to more features greater than 5 nm in height, indicative of substantial aggregation (bundling) of the SWCNTs, yet putting numbers on these differences appears to be very difficult.

Some representative cross sections from Figure 1a (numbered white lines) are shown in Figure 1e. While the SWCNTs used to make the dispersions used here have a

DOI: 10.1021/acs.langmuir.6b02475
Langmuir XXXX, XXX, XXX−XXX

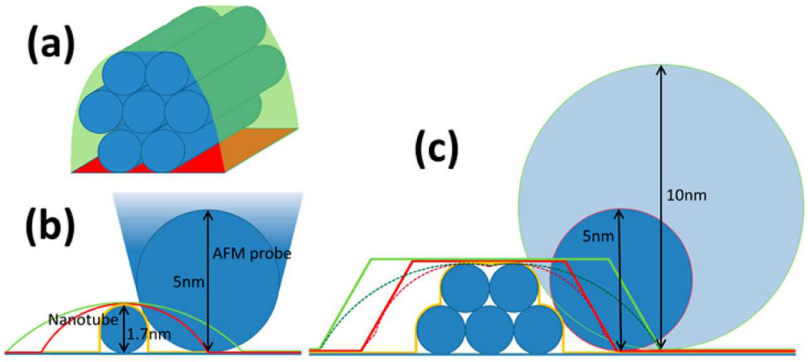

(d)

AFM tip diameter (nm) →	3	5	10	De-convolved	
Bundles and assumed AFM tip trajectories	Bundle to single nanotube AFM volume ratio $V_{Bundle\ AFM} / V_{Single\ nanotube\ AFM}$				Bundle height (nm)
	1	1	1	1	1.7
	3.41	3.33	3.37	5.1	3.2
	5.69	5.44	5.34	9.0	4.6
	10.26	9.39	8.66	17.9	6.1

Figure 2. (a) Scheme showing a bundle of seven nanotubes. The bundle's projected AFM surface is shown in red, and together with the green surface on the top it illustrates the boundaries within which the volume of the bundle is calculated. (b) Cross section showing a 1.7 nm diameter nanotube being scanned by a 5 nm diameter AFM probe. The red line corresponds to the trajectory of the lowest point of the tip during scanning. The green line shows a similar trajectory that would result from a 10 nm diameter AFM tip scanning the same nanotube, and the orange line shows the ideally deconvoluted trajectory. (c) Trajectories for the 5 and 10 nm diameter AFM tips are shown in dashed red and green lines, the ideal deconvoluted contour is shown in orange, and the trapezoid shaped approximated contours that we used in calculations carried out in panel d are shown in solid red and green lines. (d) Table based on dividing the calculated AFM volume of a bundle by the calculated AFM volume of a single nanotube for three different AFM tip diameters as well as for deconvoluted AFM images. The table highlights the error of the volume based analysis if the deconvolution is not applied.

narrow distribution of diameters ranging from 1.2 to 1.4 nm, simple geometric analysis shows that if there was no polymer wrapped and we took the three smallest 1.2 nm diameter nanotubes and bundled them together into a tight pack as illustrated in the Supporting Information Figure S1 (i), the bundle height would still not exceed 2.24 nm. On the basis of this, network features whose height is above 2 nm are considered to be bundles consisting of several nanotubes with some degree of vertical stacking, while features whose height is <2 nm are assumed to be individual SWCNTs (also see part 1 of Supporting Information). With this assumption, the analysis of cross sections in our AFM images indicates that the presence of the PFDD polymer increases the average single nanotube diameter to 1.7 nm, with the height distribution of isolated nanotubes ranging from 1.4 to 2 nm (data not shown, based on the analysis of the AFM measured height of 120 individual nanotubes rinsed with toluene). To illustrate this, profiles 2, 4, and 6 in Figure 1e, whose height is close to 1.7 nm, correspond to single or laterally aligned nanotubes and not to bundles. On the contrary, profiles 1, 3, 5, and 7, with heights clearly exceeding 2 nm, are considered to be bundles. This simple analysis indicates that for these networks many of the features seen in the AFM images are in fact bundles of more than one tube, and simple counting of features will underestimate the tube density. The remainder of this article focuses on developing a method that allows quantifying the morphology of these networks by extracting meaningful parameters from these images. These parameters can then be used to compare different network fabrication process and correlate resulting morphologies with properties of the networks.

Volumetric AFM Analysis for Carbon Nanotube Networks. Volumetric analysis of AFM data has been proposed in the past, but it was based on an apparent mass−volume relationship[15] and did not offer adequate solutions for high surface density, partly overlapping, or bundled samples. In this work, we present a volumetric analysis method that does not rely on any mass−volume equivalency and which works well even for dense and highly bundled samples. Using carbon nanotube networks, we show how this volume-based analysis can quantify the degree of bundling and offer a straightforward analysis method for a dense network, where it is often impossible to make out individual nanotubes. As discussed above (and also highlighted in the part 1 of the Supporting Information), a particular challenge when trying to quantify nanotube assemblies is the tendency for individual tubes to bundle. Even with the use of polymers to disperse the nanotubes, most of the SWCNTs in a realistic network are observed to be bundled.

The method proposed here is based on a simple hypothesis that the volume of a bundle of nanotubes is equal to the product of the volume of a single nanotube by the number of nanotubes in the bundle

$$V_{\text{bundle of N nanotubes}} = N \times V_{\text{single nanotube}} \quad (1)$$

DOI: 10.1021/acs.langmuir.6b02475
Langmuir XXXX, XXX, XXX−XXX

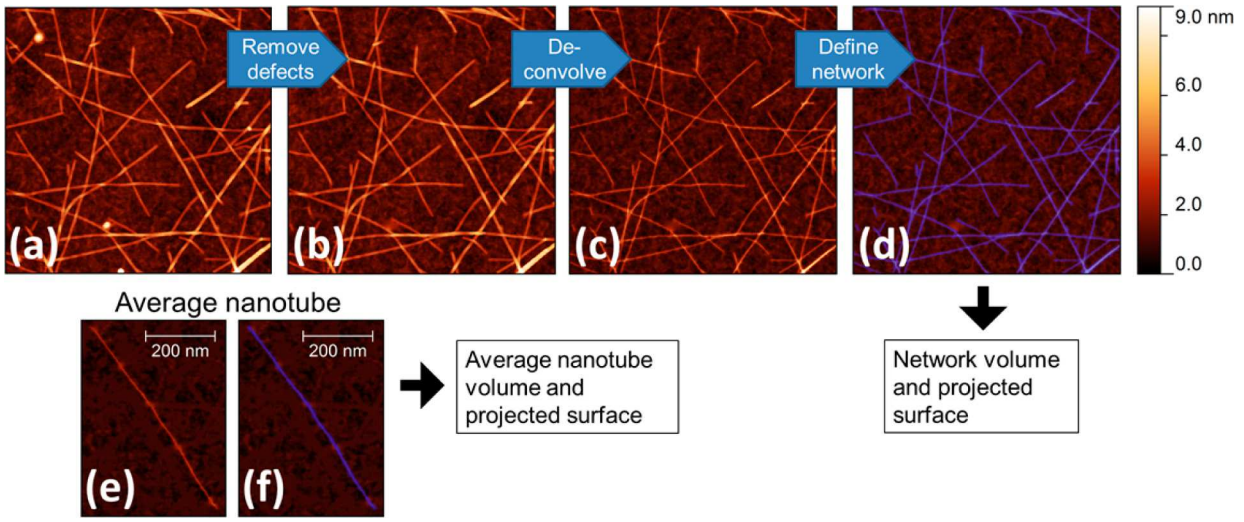

Figure 3. Analysis method outline based on the Gwyddion SPM analysis software: (a) Flattened image of a nanotube network. (b) Network defects such as non-nanotube contaminants were removed using "Small defect interpolation". (c) A tip-deconvoluted image was obtained using "Surface reconstruction" function and an estimate of the tip diameter based on the value of the tip−substrate van der Waals interaction. (d) Network is defined by setting a height threshold to define a mask (in blue) such that both the amount of blue bleeding onto the substrate and the amount of network that is not colored blue are minimized. To complete the analysis, we analyzed a single average nanotube in the same way ((e) deconvoluted and flattened and (f) masked average nanotube), and its volume and projected surface are used to normalize the network data to extract the equivalent nanotube surface density and the degree of bundling. All images are displayed at the same 9 nm vertical scale and have a pixel density of 512 × 512 pixels par μm^2. Panels a−d show 1 μm^2 of the network's surface.

Calculations to assess the validity of this hypothesis are summarized in Figure 2.

Practically, we propose to use AFM images to measure the volume of the entire network in an AFM image and then to divide it by the volume of a single, average nanotube, thus determining the number of equivalent SWCNTs in the image. Upon analyzing lengths and diameters of 30 single nanotubes (with height <2 nm and for which we could unambiguously distinguish both ends), the average nanotube length was determined to be 700 nm and the average diameter was 1.7 nm. The representative nanotube with dimensions close to these average values is shown in Figure 3e, and it was this nanotube that was used to obtain the single nanotube volume and projected surface used in the analysis later on. Upon determining the number of nanotubes in an image, the density can be easily expressed as this number divided by the total image surface.

In general, it is difficult to determine the exact number of tubes in a bundle. We propose a simple approach to quantify the degree of vertical bundling that uses the fact that upon bundling the volume of the bundle increases at a significantly higher rate than the projected surface of the bundle. Figure 2a shows a cartoon depicting a bundle of seven nanotubes, and the red surface underneath indicates schematically how its projected surface would look in the AFM image. The projected surface of this seven nanotube bundle is actually barely bigger than the projected surface of just three aligned nanotubes, yet its volume is much larger. Using this, one can define a parameter C_B that we will call the bundling coefficient

$$C_B = 1 - \frac{S_{Net}}{\frac{V_{Net}}{V_{1CNT}} \times S_{1CNT}} \quad (2)$$

In eq 2, S_{Net} is the projected network surface, V_{Net} is its volume, V_{1CNT} is the volume of the average single nanotube, and S_{1CNT} is its projected surface. The bundling coefficient defined by the eq 2 is a number between 0 and 1, where 0 means that there is no bundling (moreover, for $C_B = 0$ all of the nanotubes would have to lie on the surface without even crossing over each other), and 1 is the limit value that would be approached if all the nanotubes were stacked one on top of each other in a single vertical bundle. This coefficient is not the exact fraction of bundled nanotubes but rather an indication of the degree of vertical bundling where low C_B values (closer to 0) indicate low rates of bundling and high C_B values (closer to 1) indicate significant bundling. The comparison of C_B for two samples prepared using different protocols would clearly demonstrate which protocol leads to more or less bundling.

Deconvolution to Minimize the AFM Tip Size Effects. In Figure 2a, the volume of a bundle, as measured using the AFM, is shown as the volume enclosed by the green surface from above (larger than the actual nanotubes volume due to the AFM tip shape and the resulting tip-size-dependent convolution) and the red surface underneath. In general, the size of a feature in an AFM image is always affected by the convolution resulting from the shape of the tip. This is illustrated in Figure 2b, where the trajectory of the lowest point of a 5 nm diameter AFM tip is shown in red when scanning a 1.7 nm diameter nanotube. This trajectory represents an ideal AFM image, where the tip gets in contact with the sample without compressing or modifying it in any way. The scheme in Figure 2b shows that, even with this relatively sharp tip, the convolution effect is significant, essentially tripling the volume of a single nanotube. With a larger 10 nm diameter tip (green trajectory) the resulting convolution error becomes even more significant. A general rule is that the tip convolution becomes more substantial with increasing tip size and decreasing tube diameter. Because the sharpest commercially available AFM tips are in the 2 to 4 nm radius range and the average diameter of our nanotubes is 1.7 nm, the tip-related convolution will likely be significant in AFM images. Furthermore, the convolution effect is not equally affecting single nanotubes

DOI: 10.1021/acs.langmuir.6b02475
Langmuir XXXX, XXX, XXX−XXX

and nanotube bundles of different sizes. In Figure 2 the table (panel d) shows an estimate of the convolution effect as a function of both the tip size (calculations for 3, 5, and 10 nm tip diameters) and the bundle size (1, 5, 9, and 18 nanotube bundles). The data in the table (panel d) are obtained by calculating volumes of a single nanotube as imaged with varying size tips (the calculation is based on the assumption that the tip is in contact with the sample and that no deformations occur during imaging) and then calculating volumes of the bundles imaged with the same tips. For each tip size, the calculated bundle volume was divided by the calculated single nanotube volume, and the resulting number is shown in an appropriate tip-size column (color coded, black for the 3 nm tip, red for the 5 nm tip, and green for the 10 nm tip). The results show that convolution with an AFM tip of a realistic size always leads to an underestimation of the number of nanotubes in a bundle when performing the volumetric analysis. For example, when the AFM measured volume of a bundle composed of five nanotubes is divided by the AFM measured volume of a single nanotube, both being imaged using a 10 nm diameter tip, the result is 3.37, when it should be 5. Calculations show that, as expected, smaller tips lead to slightly less error in the volume-based estimation, whereas the error is greater for larger bundles. For example, for an 18 tube bundle measured with a 10 nm tip the error is more than 50% (8.66 instead of 18). The result was somewhat surprising, as one could expect to see the opposite trend due to all of the volume between the nanotubes in the bundles, leading to an overestimation of the number of nanotubes. However, the results demonstrate that the over-estimation of the volume of the single nanotube due to the convolution by the tip size has a much larger effect.

For the AFM−volume calculations in Figure 2, tip trajectories were always based on the assumption that the tip gets in contact with nanotubes and the substrate without deforming them. The length of the single nanotube and that of bundles are assumed to have equal values. The diameter of each of the nanotubes was set to 1.7 nm, and the nanotubes in bundles were assumed to be confluent and packed as tightly as possible, as shown in the cartoons. To simplify calculations, we approximated the tip trajectory on top of bundles to isosceles trapezoid-like trajectories, where the base of the trapezoid corresponds to the point where the tip (its side) first gets in contact with the bundle, and the angle that the trapezoid side forms with its base is 60°, as shown in Figures 2c,d. Figure 2c also shows the exact trajectories for 5 and 10 nm diameter tips with dashed lines, and one can see that the trapezoid approximation leads to a somewhat bigger bundle volume, which should lead to a larger estimated number of nanotubes, and yet the convolution effect is sufficiently significant to make this approximation error irrelevant: The actual estimated numbers of nanotubes with the trapezoid approximation are still much smaller than the actual numbers of nanotubes forming the bundles.

The orange trajectory in Figure 2c corresponds to an ideally deconvoluted trajectory. While typical deconvolution algorithms may not reach this degree of surface reconstruction, they still lead to a significant improvement in the quantitative volume estimation. We have used the Gwyddion SPM analysis software deconvolution erosion algorithm, which is well described,[14] and appears to perform well (all of the deconvoluted images corresponding to raw images in Figure 1 are shown in the Supporting Information part 3). The orange column in Figure 2d shows that deconvolution leads to recovering very accurate data based on volumetric analysis. An example of how the deconvolution software affects the image is also shown in Figure 3, where panel b shows a network image prior to and panel c shows it after the deconvolution. In all of the examples shown here the deconvolution was performed using the "surface reconstruction" function in Gwyddion (Data Process → Tip → Surface Reconstruction). This is an erosion algorithm based on a probe−sample interaction modeling that uses a purely geometrical approach. The choice of the tip model is essential for the deconvolution, where both the shape and the size of the tip have the most significant impact on the final deconvoluted image. In-depth discussion on how the most realistic tip size was determined is presented in the Supporting Information part 2. The exact settings that we have chosen to model the tip were a "pyramid" tip with 24 sides with an angle of 20° and the radius that was determined using the van der Waals force-based tip radius estimation described in part 2 of the Supporting Information and here below.

A certain amount of statistics is necessary and several areas have to be imaged to take into account regional sample heterogeneity to get quantitative and reliable data on nanotube networks. If different preparation methods are compared, the same procedure has to be done for each different network, and it is likely that several AFM probes will be used in the process or that the probe used is going to undergo some amount of degradation, which typically translates into larger tip size as the imaging progresses. To have a reliable comparison of data acquired with different probes, or with the same probe that gradually degrades with time, it is important to deconvolute the images using the size of the tip when imaging was done.

There are several ways to determine the tip radius at the time of the image acquisition: (1) imaging of an appropriate test sample before and after the network imaging; (2) imaging of well-characterized fiducial marker that would have to be deposited together with the sample of interest; (3) blind tip estimation, where the analysis software uses the actual network image to try determining the tip's shape and size; and (4) recording and using van der Waals tip−sample interactions to calculate the tip size.

While each of the above tip-size determination methods has its own drawbacks and advantages, we have opted to use the van der Waals based method, which may not be the most precise one but is timely and minimally invasive, and therefore the most practical one in our view. The calculation assumes that the tip has a spherical shape and uses the fact that the van der Waals force between a spherical tip and a planar substrate is directly proportional to the tip diameter (see details in the Supporting Information part 2).

Application of Analysis Procedure. Gwyddion SPM analysis software offers a straightforward way of calculating the network volume as well as the volume of an average nanotube, and we have broken the optimal procedure to do this into the simple steps shown in the Figure 3. Figure 3a shows an AFM image that has been flattened using a polynomial fitting of the substrate. To have only the volume and projected surface of the network, without including eventual "contaminants" (e.g., unbound polymer, catalyst particles, amorphous carbon, or other random contaminants), we eliminated any non-nanotube like features from the image prior to further analysis. Our samples appear relatively clean in general, and the contaminants that we are talking about are usually a couple of small roundish features similar to those that can be seen in Figure 3a. There is a variety of ways to do this, but we found that Gwyddion's

DOI: 10.1021/acs.langmuir.6b02475
Langmuir XXXX, XXX, XXX−XXX

Table 1. Results of the Volumetric Analysis of AFM Images of SWCNT Networks Prepared by Different Methods and Shown in Figure 1

	Piranha, toluene	Piranha, tol+THF+IPA	plasma, toluene	HOPG, toluene
nanotubes per μm^2	37 ± 8	44 ± 4	70 ± 14	52 ± 8
bundling coefficient	0.29 ± 0.03	0.61 ± 0.02	0.41 ± 0.01	0.49 ± 0.03

"remove spots" tool, which uses the "hyperbolic flatten" function to interpolate selected parts of the image, is particularly effective. Figure 3b shows the result of such a removal of several small contaminants that were present in panel a. Figure 3c shows the deconvoluted image. Finally, we have selected a height threshold that instructs the software that any part of the image that is higher than that value is a part of the network, and anything lower is the substrate. This is done by using Gwyddion's "mark grains by threshold" function, and the resulting network is shown in blue (Figure 3d). If the threshold is chosen too low, much of the substrate will appear in blue, too, particularly for rough substrates. The flatter the substrate, the more accurate the threshold choice becomes. If too high a threshold value is chosen, parts of the nanotubes that form the network, or the nanotube edges, will not be blue and will therefore not be included in the calculation of the volume. The threshold selection part of the analysis is a critical part for getting a reliable and reproducible volumetric analysis. This is the biggest contributor to the uncertainties associated with the parameters extracted using our volumetric analysis method.

Once the network versus substrate parts of the image are defined, it is straightforward to get the total network volume and its projected surface by clicking on "Distributions of grain characteristics" button in the Gwyddion main menu. We chose to have the volume calculated using "Laplacian background basis", where Gwyddion interpolates eventual surrounding substrate topography variations from the network volume to get more accurate results. The part of the analysis relying on the Gwyddion software is explained in detail in a software-supporting publication.[14]

To complete the analysis, we performed the same cleanup/deconvolution/network-definition procedure on an individual average nanotube, and Figure 3e,f show the average nanotube before and at the end of analysis, respectively. As a reminder, the average nanotube here was selected by analyzing lengths and cross sections of 30 individual tubes in networks of the same solution dispersed on silicon oxide and rinsed with toluene. This resulted in the average length and diameter of, respectively, 700 and 1.7 nm. Finally, the volume of the network is divided by the volume of the single nanotube to obtain the number of equivalent tubes contained in the network. This value is then divided by the entire surface of the image of the network, resulting in the network density. Then, eq 2 is used to calculate the bundling coefficient.

Using the volumetric analysis outlined in detail above, the SWCNT density and bundling coefficient are calculated for the four different networks shown in Figure 1, with the results summarized in Table 1. The quantitative results confirm some of the qualitative observations discussed above. For example, comparing the networks on Piranha- and plasma-cleaned silicon dioxide, the SWCNT density is almost twice as large in the latter. Perhaps less obviously, the SWCNT density for the networks in Figure 1a,b are quite similar, with the main difference between these networks being a large increase in the bundling coefficient associated with the additional rinsing steps. The ability to quantify these morphology differences by the approach outlined above will enable the correlation of process details with resulting network structures and ultimately with the properties of the nanomaterial. Although some of the results reported here could be obtained on less dense networks by patient drawing of cross sections and counting of individual tubes, the method proposed here offers a more general and time effective means to extract these parameters.

AFM Height Reliability Test. An aspect of AFM imaging that has drawn scrutiny is the reliability of the height data.[22,23] The height of nanoscale objects measured by AFM is often smaller than the true value. There are several reasons that can lead to this height underestimation, the most commonly evoked one being that the AFM probe compresses the sample during scanning. If the measured heights underestimate the real height, this would negatively impact the reliability of the volume based analysis proposed here. To verify the reliability of the AFM height measurements, we used a simple test involving successive imaging of the same network area using increasing peak force set points. Figure 4 shows the results from one such test where the same network area was scanned five times, starting at a peak force set point of 0.5 nN (image shown in

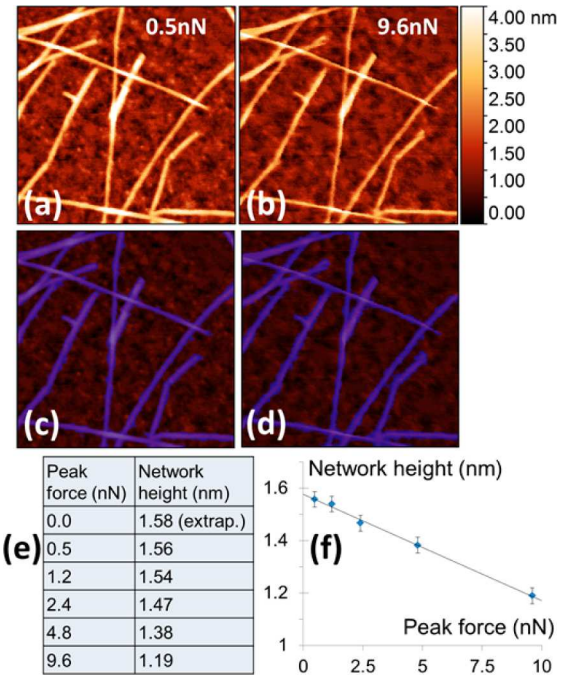

Peak force (nN)	Network height (nm)
0.0	1.58 (extrap.)
0.5	1.56
1.2	1.54
2.4	1.47
4.8	1.38
9.6	1.19

Figure 4. AFM height depends on the peak force applied by the tip during imaging: (a,b) Representative 300 × 300 nm^2 images of the same area of a nanotube network acquired with a different peak force of (a) 0.5 and (b) 9.6 nN. (c,d) The same AFM images that are shown in panels a and b but we show in blue all of the network pixels that were used to calculate the average network height. That height is shown as a function of force in panels e and f for a range of five different peak force feedback values. In panel f the height data was fitted with a straight line, and the line value at 0 force is used to extrapolate the average network height shown in the first line of the table (e).

DOI: 10.1021/acs.langmuir.6b02475
Langmuir XXXX, XXX, XXX−XXX

Figure 4a) and ending with a peak force set point of 9.6 nN (Figure 4b). Careful comparison of the two images (displayed with the same vertical scale) indicates that the nanotubes appear slightly lower at the higher set point.

To analyze these images a height threshold value was chosen, as discussed above, to separate the network from the substrate. The result of defining this mask is shown in blue in Figure 4c,d. The average network height was then calculated as the average of the heights of all pixels in the masked area minus the average height of all the unmasked pixels (the substrate). The uncertainty on the height threshold results in the error bars shown in Figure 4f. Similar data were acquired a dozen times on different areas and on different samples with the same trend being observed, although absolute values vary to some extent. The measured height exhibits a linear decrease as the force increases. Fitting the height versus compression force curve with a straight line enables extrapolation of the measured height in the absence of applied force, as shown in the Figure 4f.

For all images shown in Figure 1, we used the same peak force feedback value of 0.5 nN. The average network height at this force feedback as extracted from the image in Figure 4a is 1.56 nm. This is lower than the average individual nanotube diameter because this value takes into account all of the blue pixels and not just the ones that are on top of nanotubes that matter in the diameter calculation. (The height of pixels on sides of nanotubes and close to the substrate is taken into account in this average network height calculation.) This is very close to the extrapolated height at zero force of 1.58 nm. The small (0.02 nm) difference between the measured height under typical imaging settings and that at zero force demonstrates that interactions with the tip are not significantly affecting our measurements of the SWCNT networks. However, this easy-to-do test does show that there is indeed a reduction in apparent height with increasing force, which could introduce significant errors in a volume-based quantitative analysis of the network morphology. Therefore, as part of such an analysis it is best to run a similar test to find the force range that does not significantly perturb the height measurements.

SUMMARY AND CONCLUSIONS

The development of process−structure−property relationships in materials constructed from nanoscale building blocks requires methods for quantitative assessment of often complex sample morphologies. The volume-based approach for analyzing AFM images of random nanotube networks presented here allows going beyond qualitative statements regarding network morphologies and facilitates extraction of two important parameters, the SWCNT density and the bundling coefficient.

For these networks, where morphology is expected to play an important role in influencing the electrical transport properties, these parameters should be useful in guiding the optimization of processes for solution-based fabrication of transparent conducting films and TFTs. We are currently using the approach developed here to analyze the morphology of SWCNT TFTs to determine how the morphological parameters correlate with electrical performance. It is expected that such studies will provide insight into how morphology influences device behavior, particularly with respect to the role of bundling, which has not yet been systematically investigated.

Beyond the specific case of random networks of SWCNTs, which were used here to develop and illustrate the analysis method, this approach should be widely applicable to other nanomaterial systems. It is particularly useful in cases where significant aggregation of the nano-objects makes it difficult to use simple counting approaches to determine the density.

ASSOCIATED CONTENT

Supporting Information

The Supporting Information is available free of charge on the ACS Publications website at DOI: 10.1021/acs.langmuir.6b02475.

AFM images with cross sections showcasing the bundling of polymer dispersed carbon nanotubes, AFM tip size estimation and deconvolution procedure, deconvoluted images, uncertainty analysis based on height threshold to separate nanotubes from the substrate, and references. (PDF)

AUTHOR INFORMATION

Corresponding Author

*E-mail: dusan.vobornik@nrc.ca.

Notes

The authors declare no competing financial interest.

ACKNOWLEDGMENTS

We thank Dr. Brian Eves for discussions and advice concerning the accuracy of the AFM height measurement and Dr. Christa Homenick, Dr. Paul Finnie, and Dr. Jacques Lefebvre for sharing their nanotube networks preparation experience. This work was supported by NRCs Measurement Science for Emerging Technologies Program.

REFERENCES

(1) Jariwala, D.; Sangwan, V. K.; Lauhon, L. J.; Marks, T. J.; Hersam, M. C. Carbon Nanomaterials for Electronics, Optoelectronics, Photovoltaics, and Sensing. *Chem. Soc. Rev.* **2013**, *42*, 2824−2860.

(2) Novoselov, K. S.; Fal'ko, V. I.; Colombo, L.; Gellert, P. R.; Schwab, M. G.; Kim, K. A Roadmap for Graphene. *Nature* **2012**, *490* (7419), 192−200.

(3) Holzinger, M.; Le Goff, A.; Cosnier, S. Nanomaterials for Biosensing Applications: A Review. *Front. Chem.* **2014**, *2* (August), 63.

(4) Park, S.; Vosguerichian, M.; Bao, Z. A Review of Fabrication and Applications of Carbon Nanotube Film-Based Flexible Electronics. *Nanoscale* **2013**, *5* (5), 1727−1752.

(5) Islam, A. E.; Rogers, J. A.; Alam, M. A. Recent Progress in Obtaining Semiconducting Single-Walled Carbon Nanotubes for Transistor Applications. *Adv. Mater.* **2015**, *27* (48), 7908−7937.

(6) Che, Y.; Chen, H.; Gui, H.; Liu, J.; Liu, B.; Zhou, C. Review of Carbon Nanotube Nanoelectronics and Macroelectronics. *Semicond. Sci. Technol.* **2014**, *29* (1−17), 073001.

(7) Zaumseil, J. Single-Walled Carbon Nanotube Networks for Flexible and Printed Electronics. *Semicond. Sci. Technol.* **2015**, *30* (7), 074001.

(8) Hecht, D.; Hu, L.; Grüner, G. Conductivity Scaling with Bundle Length and Diameter in Single Walled Carbon Nanotube Networks. *Appl. Phys. Lett.* **2006**, *89*, 133112.

(9) Lee, J.; Stein, I. Y.; Devoe, M. E.; Lewis, D. J.; Lachman, N.; Kessler, S. S.; Buschhorn, S. T.; Wardle, B. L. Impact of Carbon Nanotube Length on Electron Transport in Aligned Carbon Nanotube Networks. *Appl. Phys. Lett.* **2015**, *106*, 053110.

(10) Lyons, P. E.; De, S.; Blighe, F.; Nicolosi, V.; Pereira, L. F. C.; Ferreira, M. S.; Coleman, J. N. The Relationship between Network Morphology and Conductivity in Nanotube Films. *J. Appl. Phys.* **2008**, *104*, 044302.

(11) Gupta, M. P.; Behnam, A.; Lian, F.; Estrada, D.; Pop, E.; Kumar, S. High Field Breakdown Characteristics of Carbon Nanotube Thin Film Transistors. *Nanotechnology* **2013**, *24* (40), 405204.

DOI: 10.1021/acs.langmuir.6b02475
Langmuir XXXX, XXX, XXX−XXX

(12) Timmermans, M. Y.; Estrada, D.; Nasibulin, A. G.; Wood, J. D.; Behnam, A.; Sun, D.-m.; Ohno, Y.; Lyding, J. W.; Hassanien, A.; Pop, E.; et al. Effect of Carbon Nanotube Network Morphology on Thin Film Transistor Performance. *Nano Res.* **2012**, *5* (5), 307−319.
(13) Liu, Z.; Zhao, J.; Xu, W.; Qian, L.; Nie, S.; Cui, Z. Effect of Surface Wettability Properties on the Electrical Properties of Printed Carbon Nanotube Thin-Film Transistors on SiO2/Si Substrates. *ACS Appl. Mater. Interfaces* **2014**, *6* (13), 9997−10004.
(14) Klapetek, P.; Valtr, M.; Nečas, D.; Salyk, O.; Dzik, P. Atomic Force Microscopy Analysis of Nanoparticles in Non-Ideal Conditions. *Nanoscale Res. Lett.* **2011**, *6* (1), 514.
(15) Fuentes-Perez, M. E.; Dillingham, M. S.; Moreno-Herrero, F. AFM Volumetric Methods for the Characterization of Proteins and Nucleic Acids. *Methods* **2013**, *60* (2), 113−121.
(16) Japaridze, A.; Vobornik, D.; Lipiec, E.; Cerreta, A.; Szczerbinski, J.; Zenobi, R.; Dietler, G. Toward an Effective Control of DNA's Submolecular Conformation on a Surface. *Macromolecules* **2016**, *49* (2), 643−652.
(17) van Raaij, M. E.; van Gestel, J.; Segers-Nolten, I. M. J.; de Leeuw, S. W.; Subramaniam, V. Concentration Dependence of Alpha-Synuclein Fibril Length Assessed by Quantitative Atomic Force Microscopy and Statistical-Mechanical Theory. *Biophys. J.* **2008**, *95* (10), 4871−4878.
(18) Baalousha, M.; Prasad, a; Lead, J. R. Quantitative Measurement of the Nanoparticle Size and Number Concentration from Liquid Suspensions by Atomic Force Microscopy. *Environ. Sci. Process. Impacts* **2014**, *16* (6), 1338−1347.
(19) Grobelny, J.; Delrio, F. W.; Pradeep, N.; Kim, D.; Hackley, V. A.; Cook, R. F. Characterization of Nanoparticles Intended for Drug Delivery. In *Characterization of Nanoparticles Intended for Drug Delivery*; McNeil, S. E., Ed.; Methods in Molecular Biology; Humana Press: Totowa, NJ, 2011; Vol. *697*, pp 71−82.
(20) Ding, J.; Li, Z.; Lefebvre, J.; Cheng, F.; Dubey, G.; Zou, S.; Finnie, P.; Hrdina, A.; Scoles, L.; Lopinski, G. P.; et al. Enrichment of Large-Diameter Semiconducting SWCNTs by Polyfluorene Extraction for High Network Density Thin Film Transistors. *Nanoscale* **2014**, *6* (4), 2328−2339.
(21) Nečas, D.; Klapetek, P. Gwyddion: An Open-Source Software for SPM Data Analysis. *Open Phys.* **2012**, *10* (1), 181−188.
(22) Santos, S.; Barcons, V.; Christenson, H. K.; Font, J.; Thomson, N. H. The Intrinsic Resolution Limit in the Atomic Force Microscope: Implications for Heights of Nano-Scale Features. *PLoS One* **2011**, *6* (8), e23821.
(23) Deborde, T.; Joiner, J. C.; Leyden, M. R.; Minot, E. D. Identifying Individual Single-Walled and Double-Walled Carbon Nanotubes by Atomic Force Microscopy. *Nano Lett.* **2008**, *8*, 3568−3571.

DOI: 10.1021/acs.langmuir.6b02475
Langmuir XXXX, XXX, XXX−XXX